LETTERS

Transformation of spin information into large electrical signals using carbon nanotubes

Luis E. Hueso[1]†, José M. Pruneda[2,3]†, Valeria Ferrari[4]†, Gavin Burnell[1]†, José P. Valdés-Herrera[1,5], Benjamin D. Simons[4], Peter B. Littlewood[4], Emilio Artacho[2], Albert Fert[6] & Neil D. Mathur[1]

Spin electronics (spintronics) exploits the magnetic nature of electrons, and this principle is commercially applied in, for example, the spin valves of disk-drive read heads. There is currently widespread interest in developing new types of spintronic devices based on industrially relevant semiconductors, in which a spin-polarized current flows through a lateral channel between a spin-polarized source and drain[1,2]. However, the transformation of spin information into large electrical signals is limited by spin relaxation, so that the magnetoresistive signals are below 1% (ref. 2). Here we report large magnetoresistance effects (61% at 5 K), which correspond to large output signals (65 mV), in devices where the non-magnetic channel is a multiwall carbon nanotube that spans a 1.5 μm gap between epitaxial electrodes of the highly spin polarized[3,4] manganite $La_{0.7}Sr_{0.3}MnO_3$. This spintronic system combines a number of favourable properties that enable this performance; the long spin lifetime in nanotubes due to the small spin–orbit coupling of carbon; the high Fermi velocity in nanotubes that limits the carrier dwell time; the high spin polarization in the manganite electrodes, which remains high right up to the manganite–nanotube interface; and the resistance of the interfacial barrier for spin injection. We support these conclusions regarding the interface using density functional theory calculations. The success of our experiments with such chemically and geometrically different materials should inspire new avenues in materials selection for future spintronics applications.

We show how carbon nanotubes (CNTs) can solve a long-standing spintronics challenge—namely, the injection of spins into a non-magnetic material and the subsequent transformation of the spin information into a large electrical signal. This challenge began in 1990 with the introduction[5] of the spin-transistor concept. The idea is to use a gate voltage to manipulate spins injected into a semiconductor channel between ferromagnetic contacts. In all spin-transistor concepts based on similar structures[1,2], the prerequisite is a significant magnetoresistance ($MR = \Delta R/R_P$) of the order of unity or larger, where $\Delta R = R_{AP} - R_P$ is the resistance change when a magnetic field alters the relative orientation of the magnetizations of source and drain electrodes between antiparallel (AP) and parallel (P). Experimental MR values[2] have been limited to ~0.1–1%. Here we show why replacing the semiconductor channel with a CNT permits a value of MR = 61%, and thus a significant voltage change of 65 mV.

CNTs are robust, easy to manipulate, and have been successfully used[6] in proof-of-principle field-effect transistors, quantum dots and logic gates. For spintronics, the weak spin–orbit coupling permits a long spin lifetime. Here we also exploit the large[7] CNT Fermi velocity v_F, related to the zero bandgap character of the electronic structure and the resulting linear dispersion[6]. However, it is far from obvious whether spin information can survive long-distance transport, given the likelihood of defects and contamination.

Our study of CNTs with ferromagnetic electrodes represents a fusion of molecular[8] and spin electronics[1], that is, molecular spintronics. In this nascent field, MR effects are typically confined to low temperatures in devices based on octanethiol[9], C_{60} (ref. 10) or CNTs[11–14]. These CNT devices used electrodes made of cobalt[11,14], Pd-Ni (ref. 12) or GaMnAs (ref. 13), and MR effects were studied at low biases and temperatures. The MR is generally small (~10%), and inversions of sign, either from sample to sample, or as a function of voltage[11–14], are related to Coulomb blockade and level quantization. We avoid these effects by measuring MR up to 120 K, and under biases exceeding 25 mV. This voltage is sufficient, given that the Coulomb blockade energy[7] for similar CNTs with albeit different contacts is ~0.1 meV, and given also a level spacing of $hv_F/2L \approx 0.8$ meV for an undoped metallic tube of length $L = 2\,\mu m$ with $v_F = 0.8 \times 10^6\ m\,s^{-1}$ (ref. 7). High-bias MR measurements are possible because naturally occurring tunnel barriers at each electrode–CNT interface limit the current and thus unwanted heating, and significant because unlike MR values alone they represent large output signals.

In this Letter, we present devices (Fig. 1 and Methods) in which epitaxial electrodes of the pseudo-cubic perovskite manganite $La_{0.7}Sr_{0.3}MnO_3$ (LSMO) are electrically connected by a single multiwall CNT, which lies on top of the electrodes—in contrast to standard nanotube device geometries[6]. At low temperatures, the conduction in LSMO exhibits a very high spin polarization[3,4] approaching 100%, whereas the figure for elemental ferromagnets[15] is <40%. Moreover, as LSMO is an oxide, it displays environmental stability, so molecules may be introduced *ex situ*. However, it is not *a priori* known whether spin information can be efficiently transmitted between two materials that possess very different geometries and chemistries.

Similar and reproducible zero-field current–voltage (I–V) characteristics (Supplementary Fig. S1) were seen in 12 devices. Four of these show the large MR effects discussed later, and the other eight show no MR effects. Our CNT–LSMO interfaces behave like tunnel junctions in two respects: first, the $I(V)$ curves are strongly nonlinear; and second, the low-bias (25 mV), low-temperature (5 K) resistance V/I = 10–100 MΩ of our 12 devices is 3–4 orders of magnitude larger than the inverse of the quantum conductance e^2/h typically seen[12,14,16]

[1]Department of Materials Science, University of Cambridge, Pembroke Street, Cambridge CB2 3QZ, UK. [2]Department of Earth Sciences, University of Cambridge, Downing Street, Cambridge CB2 3EQ, UK. [3]Institut de Ciencia de Materials de Barcelona, CSIC Campus UAB, 08193 Bellaterra, Barcelona, Spain. [4]Cavendish Laboratory, University of Cambridge, JJ Thomson Avenue, Cambridge CB3 0HE, UK. [5]Nanoscience Centre, University of Cambridge, JJ Thomson Avenue, Cambridge CB3 0FF, UK. [6]Unité Mixte de Physique CNRS-Thales, TRT, 91767 Palaiseau and Université Paris-Sud, 91405 Orsay, France. †Present addresses: ISMN-CNR, via Gobetti 101, 40129 Bologna, Italy (L.E.H.); Department of Physics, University of California, Berkeley, California 94720, USA (J.M.P.); Departamento de Física, Comisión Nacional de Energia Atómica, Gral. Paz 1499, 1650 San Martín, Buenos Aires, Argentina (V.F.); School of Physics and Astronomy, University of Leeds, Leeds LS2 9JT, UK (G.B.).

for nanotubes between standard metallic electrodes (~13 kΩ). Note that tunnel barriers are generally found at the interfaces between LSMO and metals[17]. However, the interfacial resistance of our devices[18] is not unduly high, and falls within the wide range of values[17] associated with metal–LSMO contacts.

The observed tunnel barriers may be understood through first-principles calculations (Methods) of the electronic structure of an LSMO–CNT interface. The CNT is not significantly altered when contacted by LSMO (Fig. 2a), suggesting that the barrier is localized at the interface, and that our experiments may be insensitive to CNT type and orientation. The Kohn–Sham potential[19]—the simplest estimate of the local energy of a tunnelling electron—shows a barrier (Fig. 2 inset) whose height somewhat exceeds the characteristic CNT kinetic energy (as estimated by the inverse density of states). This is a prerequisite for a tunnel barrier, although the ratio of height to kinetic energy suggests a decay length not much smaller than the barrier width itself, and therefore a relatively high transmission probability. Note that our first-principles calculations also help explain the large MR, because they indicate (Fig. 2b) that the LSMO surface is highly spin polarized despite a pronounced interfacial state ~0.2 eV below the Fermi level.

Our main result is the observation of a large device MR value of 61% (Fig. 3) that arises because of sharp and irreversible switching of the LSMO electrode magnetizations between parallel and antiparallel. Three other working devices showed values of 54%, 72% and 53% (Supplementary Information). These four MR values are much higher than the values generally observed[11–14] with CNTs between other ferromagnetic contacts (~10%). We now discuss why the use of a CNT in place of a standard semiconductor permits the large MR.

The MR of a structure composed of a conduction channel connected to a ferromagnetic source and drain through spin-dependent interface resistances (for example, a tunnel junction) can be expressed[20,21] as:

$$\mathrm{MR} = \frac{\Delta R}{R_\mathrm{P}} \equiv \frac{R_\mathrm{AP} - R_\mathrm{P}}{R_\mathrm{P}} \equiv \frac{\gamma^2/(1-\gamma^2)}{1+\tau_\mathrm{n}/\tau_\mathrm{sf}} \quad (1)$$

where γ is the electrode spin polarization, or more formally the interfacial spin-asymmetry coefficient that influences the spin-dependent interface resistance $r_{\uparrow(\downarrow)} = 2(1 \mp \gamma)\, r_\mathrm{b}^*$ where r_b^* is the mean value of the spin-independent interface resistance, τ_sf is the spin lifetime and τ_n is the dwell time of the electrons in the channel:

$$\tau_\mathrm{n} = 2\,L/(v_\mathrm{N}\,\bar{t}_\mathrm{r}) \quad (2)$$

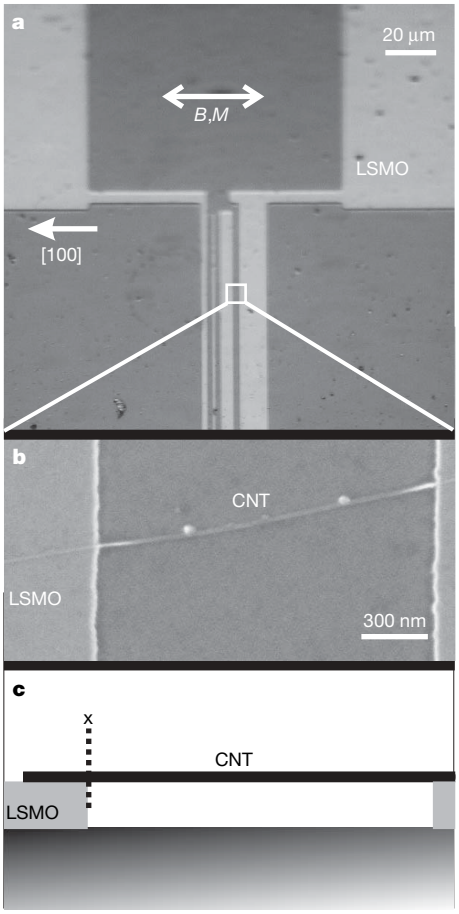

Figure 1 | LSMO–CNT–LSMO device. **a**, Optical micrograph of four variable-width LSMO electrodes, and two of the four associated contact pads. In electrically conducting devices, two adjacent electrodes were connected by an overlying CNT, in regions such as that in the white square. Magnetic fields B were applied along the orthorhombic [100] direction in which the magnetization M is expected to lie due to uniaxial magnetocrystalline anisotropy. **b**, Scanning electron microscope image of a CNT running between LSMO electrodes; magnified view corresponding to the boxed area in **a**. **c**, Schematic side view of **b** with the plane through the CNT at the edge of the LSMO electrode denoted ×.

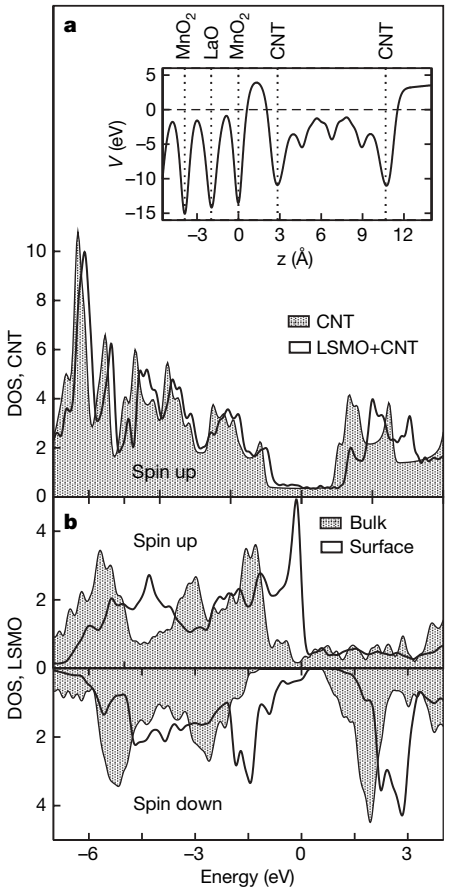

Figure 2 | First-principles calculations of device interfaces. Projected density of states (DOS) on **a**, the basis functions of an isolated CNT (shaded), and a CNT lying on LSMO (unshaded). **b**, the projected DOS onto the first MnO_2+(La,Sr)O layer of the LSMO slab (unshaded) and onto bulk LSMO (shaded). Fermi levels are aligned at zero energy, and only up spins are shown in **a** as up–down differences in the CNT DOS are barely visible at this scale (there is a net spin polarization of +0.01 electrons $Å^{-1}$). Inset, the Kohn–Sham potential seen by electrons in the vicinity of the LSMO–CNT interface. It has been integrated for each value of z (normal to the LSMO surface) in the rectangle defined by the projection of the CNT onto the x–y plane. The origin of potential has been chosen at the Fermi level (horizontal dashed line). Vertical dotted lines indicate the nuclear positions of the atomic layers of LSMO, and the limits of the CNT.

L is the channel length, v_N is the mean electron velocity in the channel (here, v_F for the CNT), and $\bar{t}_r$ is the mean interfacial transmission coefficient that we estimate later via r_b^*. Equations (1) and (2) hold for ballistic transmission from source to drain, and also for diffusive transport when r_b^* is sufficiently large[20,21], as we have here.

Equation (1) shows that MR is controlled by two factors: trivially γ, and critically τ_n/τ_{sf}. If this ratio were large, the MR would tend to zero, whatever γ. From equation (2), we can express this ratio as:

$$\frac{\tau_n}{\tau_{sf}} = \frac{2L}{v_N \bar{t}_r \tau_{sf}} \quad (3)$$

From equation (1), γ and τ_n/τ_{sf} cannot both be extracted from the MR alone (61% at 5 K, 25 mV), but we necessarily have $\gamma \geq 0.62$ as the denominator cannot be smaller than unity. It is possible that $\gamma = 1$ for half-metallic LSMO, but interfacial imperfections lead to smaller values. The maximum value observed in epitaxial magnetic tunnel junctions[4] with LSMO is 0.95. Here we propose a tentative scenario assuming a reasonable value of $\gamma = 0.8$, which gives $\tau_n/\tau_{sf} \approx 2$.

To estimate τ_{sf}, we obtain τ_n from equation (2), with $L = 2\,\mu m$, $v_N = v_F = 0.8 \times 10^6\,m\,s^{-1}$ (ref. 7) and $\bar{t}_r \approx 0.9 \times 10^{-4}$ estimated from r_b^* using the Landauer equation:

$$r_b^* = \frac{h}{4e^2 \bar{t}_r} \quad (4)$$

where the assumption of two spin-degenerate conduction channels in deriving this equation is realistic[7] even for a multiwall CNT. As r_b^* dominates device resistance R, we take $r_b^* = R/2 \approx 75\,M\Omega$. The above yields $\tau_n \approx 60$ ns, and thus $\tau_{sf} \approx 30$ ns. This value is reasonable given the very weak spin–orbit coupling of carbon, and should also apply to other carbon-based molecules. The corresponding spin diffusion length is $l_{sf} = \sqrt{v_F \tau_{sf} \lambda} \approx 50\,\mu m$, assuming a CNT mean free path[7] of $\lambda \approx 100$ nm.

Equivalent calculations with the best value[4] of $\gamma \approx 0.95$ would reduce τ_{sf} by a factor of 7 and shorten l_{sf} by a factor of 2.7. Alternatively, if hole-doping activates 10 rather than 4 CNT channels, τ_{sf} would increase by a factor of 2.5 and l_{sf} would increase by a factor of 1.6. If both scenarios are active, then clearly the former would outcompete the latter.

Purely metallic structures like magnetic multilayers have the advantage of a large carrier velocity and a large $\bar{t}_r \approx 1$, but τ_{sf} is very short so that a large $\Delta R/R$ can be obtained only when L is short—for example, in current-perpendicular-to-the-plane giant magnetoresistance. The long L in a lateral structure forces $\Delta R/R$ to become small, for example[1], ~5%. When the interfaces are tunnel junctions, in lateral structures suitable for gating, the concomitant reduction of $\bar{t}_r$ leads to an even smaller $\Delta R/R$ (for example[22], $\sim 10^{-4}$).

Semiconductors have the advantage of a long[1] τ_{sf}, but the mean velocity v_N is small. For example, n-type GaAs (carrier density $10^{17}\,cm^{-3}$) has a long low-temperature conduction-band spin lifetime of several nanoseconds, but the mean velocity along a channel axis is $\sim 3 \times 10^4\,m\,s^{-1}$, compared to $10^6\,m\,s^{-1}$ in metals or CNTs. Moreover, semiconductor channels require a small $\bar{t}_r$ for efficient spin injection from metals[23–26]. The MR < 1% of lateral semiconductor structures[2] may be increased to ~40% using a small $L \approx 5$–10 nm in vertical structures[27], but these are unsuitable for gating.

The advantage of CNTs is that they combine the long τ_{sf} of semiconductors with the large[7] v_F of metals. This permits our large MR, despite the long $L = 2\,\mu m$ and the small $\bar{t}_r$. In fact, a small $\bar{t}_r$ is necessary here to limit current at high bias. Working at high bias not only avoids Coulomb blockade and level quantization effects, but is in addition a prerequisite for achieving large output signals.

The bias dependence of the 5 K MR (Fig. 4) is reminiscent of LSMO tunnel junctions[28], but we cannot rule out the possible role of CNT energy bands here. Above the (unresolved) classical zero-bias anomaly, there is a plateau out to $V \approx 110$ mV, and then a steep decrease. The persistence of this plateau to ~110 mV permits the associated output signal (that is, the voltage difference between the parallel and antiparallel configurations for the same current) to increase from $V \times MR = 15$ mV at a bias of 25 mV, up to 65 mV at a bias of 110 mV. This figure of 65 mV falls in a suitable range for applications.

Device MR falls with increasing temperature (Fig. 4), but the field dependence is qualitatively unchanged. Our MR persists to 120 K, which, although well below room temperature, is a significant improvement on previous molecular spintronics devices[9–14]. This loss of performance well below the 365 K Curie temperature of bulk LSMO is probably associated with the well known thermal suppression of spin polarization[3]. A similar fall-off in performance in LSMO tunnel junctions[28] is attributed to a reduced interfacial Curie temperature arising from charge transfer or loss of bulk symmetry. Replacing LSMO with a high-Curie-temperature metal such as Co could solve this problem, but previous results[11–14] were limited by interfacial resistances (<1 MΩ) two orders of magnitude smaller than r_b^*, suggesting the need for tunnel barriers (for example, thin

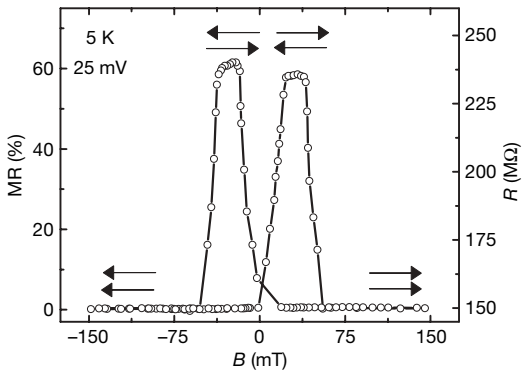

Figure 3 | MR for a LSMO–CNT–LSMO device. Data recorded at 5 K with a bias voltage of 25 mV show two distinct states of resistance R, as the magnetic configuration of the two LSMO electrodes is switched by an applied magnetic field B. The arrows indicate the relative magnetic orientation of the electrodes, which possess different switching fields because of their different widths. The data points and interconnecting lines were generated by averaging over 25 cycles; MR(%) was calculated as $MR(\%) = 100 \times [R(B) - R(0)]/R(B)$. In Supplementary Information, we show similar MR data for three other working devices. One of these three devices was fabricated with silica between the manganite electrodes to prevent the possibility of the CNT sagging. For another of these three devices, data were collected from a single field sweep.

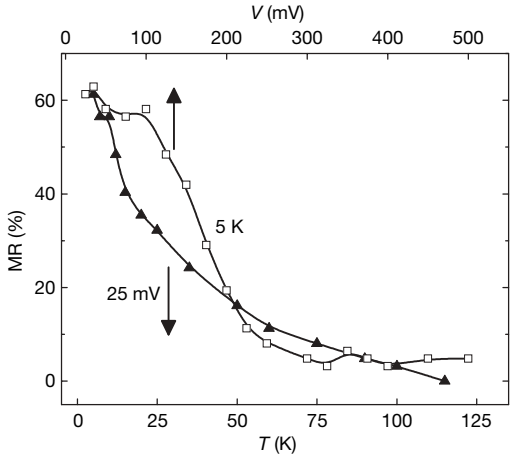

Figure 4 | Temperature and bias dependence of peak MR. The magnitude of the two-state switching seen in Fig. 4 is plotted as a function of bias voltage V at low temperature (open squares), and as a function of temperature T at 25 mV (filled triangles). MR was calculated as $MR(\%) = 100 \times [R_{AP} - R_P]/R_P$.

insulating layers) in order to limit the potentially destructive effect of current at biases sufficient to (1) avoid Coulomb blockade and level quantization effects, and (2) achieve large electrical signals.

Our work forms part of the nascent molecular spintronics approach in which it is possible to manipulate spin-polarized electrons in novel environments. However, the weak spin–orbit coupling in carbon precludes the electrically driven magnetic reversal of spins in a CNT-based spin transistor of the type described in ref. 5. Instead, spin precession induced by the local magnetic field from a ferromagnetic gate, that is, the Hänle effect[1], could be used to flip spins in a CNT. Given that the precession angle induced by a transverse field B during time t is $2\mu_B B\,t/\hbar$, our value of τ_n ($\sim$60 ns) suggests that the application of a modest 10 mT field to a small fraction of the length of a CNT (a few tenths of micrometres) would be sufficient to reverse the spin polarization between injection and detection. Note that here we cannot rule out the possibility that weak components of stray field from our LSMO electrodes reduce the MR values that we present. In future, one might seek non-magnetic channels with intermediate levels of spin–orbit coupling in order to permit spin manipulation by the electric field of a gate without unduly reducing the spin lifetime and the output signals.

METHODS

Experimental. Epitaxial LSMO thin films were grown on closely lattice matched orthorhombic $NdGaO_3$ (001) substrates by pulsed laser deposition with a KrF excimer laser (248 nm, 1 Hz, 2.5 J cm^{-2}, 775 °C, 15 Pa O_2, target–substrate distance = 8 cm). The films display step-terrace growth, and possess in-plane uniaxial magnetocrystalline anisotropy in the orthorhombic [100] direction. Below 360 K the films are ferromagnetic (3.6 μ_B per Mn at 10 K), and on cooling the resistivity decreases to $\sim$60 μΩ cm at 10 K. Using conventional photolithography, electrode tracks (widths 1–4 μm, separation 1.5 μm) were defined perpendicular to [100], so that their magnetizations could be switched independently by an external magnetic field. Multiwall CNTs of diameter $\sim$20 nm grown by arc-discharge (Iljin Nanotech) were subsequently dispersed from a 1,2-dicloroethane solution. A scanning electron microscope was used to confirm the presence of a single nanotube running between adjacent electrically connected electrodes. Electrical measurements of interest were made using a Keithley source meter in constant voltage mode.

Theoretical. First-principles electronic-structure calculations were performed within the density-functional-theory (DFT) framework[19] in the spin-polarized generalized-gradient approximation, using the SIESTA method[29]. Further details on the performance of the method for LSMO can be found elsewhere[30]. The MnO_2-terminated (001) surface of LSMO was described by a 23-layer slab of LSMO, in which one third of the La atoms where replaced[30] by Sr. A (6,6) single-wall CNT was put onto the LSMO surface in a commensurate arrangement in which three unit cells of the CNT were laid along the (100) direction on a 4×2 lateral supercell of LSMO. The mismatch strain is 5%. The atomic positions of the CNT on the previously relaxed surface were obtained by minimizing the mutual DFT forces. Even though experiments were performed on multiwall nanotubes, which are arguably better described in the graphitic limit, we have nevertheless considered a nanotube, as the dimensionality greatly affects the contact resistance, and the qualitative picture emerging from the calculations should remain.

Received 7 September; accepted 27 November 2006.

1. Žutić, I., Fabian, J. & das Sarma, S. Spintronics: Fundamentals and applications. *Rev. Mod. Phys.* **76,** 323–410 (2004).
2. Jonker, B. T. & Flatté, M. E. F. in *Nanomagnetism* (eds Mills, D. L. & Bland, J. A. C.) 227–272 (Elsevier, Amsterdam, 2006).
3. Park, J.-H. *et al.* Direct evidence for a half-metallic ferromagnet. *Nature* **392,** 794–796 (1998).
4. Bowen, M. *et al.* Nearly total spin-polarization in $La_{2/3}Sr_{1/3}MnO_3$ from tunnelling experiments. *Appl. Phys. Lett.* **82,** 233–235 (2003).
5. Datta, S. & Das, B. Electric analog of the electro-optic modulator. *Appl. Phys. Lett.* **56,** 665–667 (1990).
6. Dresselhaus, M. S., Dresselhaus, G. & Avouris, Ph (eds) *Carbon Nanotubes* (Springer, Berlin, 2001).
7. Buitelaar, M. R., Bachtold, A., Nussbaumer, T., Iqbal, M. & Schönenberger, C. Multiwall carbon nanotubes as quantum dots. *Phys. Rev. Lett.* **88,** 156801 (2002).
8. Joachim, C., Gimzewski, J. K. & Aviram, A. Electronics using hybrid-molecular and mono-molecular devices. *Nature* **408,** 541–548 (2000).
9. Petta, J. R., Slater, S. K. & Ralph, D. C. Spin-dependent transport in molecular tunnel junctions. *Phys. Rev. Lett.* **93,** 136601 (2004).
10. Pasupathy, A. N. *et al.* The Kondo effect in the presence of ferromagnetism. *Science* **306,** 86–89 (2004).
11. Tsukagoshi, K., Alphenaar, B. W. & Ago, H. Coherent transport of electron spin in a ferromagnetically contacted carbon nanotube. *Nature* **401,** 572–574 (1999).
12. Sahoo, S. *et al.* Electric field control of spin transport. *Nature Phys.* **1,** 99–102 (2005).
13. Jensen, A., Hauptmann, J. R., Nygård, J. & Lindelof, P. E. Magnetoresistance in ferromagnetically contacted single-wall carbon nanotubes. *Phys. Rev. B* **72,** 035419 (2005).
14. Tombros, N., van der Molen, S. J. & van Wees, B. J. Separating spin and charge transport in single-wall carbon nanotubes. *Phys. Rev. B* **73,** 233403 (2006).
15. Meservey, R. & Tedrow, P. M. Spin-polarized electron tunneling. *Phys. Rep.* **238,** 173–243 (1994).
16. Jorgensen, H. I., Grove-Rasmussen, K., Novotny, T., Flensberg, K. & Lindelof, P. E. Electron transport in single-wall carbon nanotube weak links in the Fabry-Perot regime. *Phys. Rev. Lett.* **96,** 207003 (2006).
17. Mieville, L., Wordledge, D., Geballe, T. H., Contreras, R. & Char, K. Transport across conducting ferromagnetic oxides/metal interfaces. *Appl. Phys. Lett.* **73,** 1736–1739 (1998).
18. Hueso, L. E. *et al.* Electrical transport between epitaxial manganites and carbon nanotubes. *Appl. Phys. Lett.* **88,** 083120 (2006).
19. Kohn, W. & Sham, L. J. Self-consistent equations including exchange and correlations effects. *Phys. Rev.* **140,** 1133–1138 (1965).
20. George, J. M. *et al.* Electrical spin injection in GaMnAs-based junctions. *Mol. Phys. Rep.* **40,** 23–33 (2004).
21. Fert, A., George, J. M., Jaffrès, H. & Mattana, R. Semiconductors between spin-polarized source and drain. *IEEE Trans. Electron. Devices* (special issue on spintronics) (in the press); preprint at ⟨http://arxiv.org/abs/cond-mat/0612495⟩ (2006).
22. Jedema, F. J., Heersche, H. B., Filip, A. T., Baselmans, J. J. A. & van Wees, B. J. Electrical detection of spin precession in a metallic mesoscopic spin valve. *Nature* **416,** 713–716 (2002).
23. Schmidt, G., Ferrand, D., Molenkamp, L. W., Filip, A. T. & van Wees, B. J. Fundamental obstacle for electrical spin injection from a ferromagnetic metal into a diffusive semiconductor. *Phys. Rev. B* **62,** 4790–4793 (2000).
24. Rashba, E. Theory of electrical spin injection: tunnel contacts as a solution of the conductivity mismatch problem. *Phys. Rev. B* **62,** 16267–16270 (2000).
25. Fert, A. & Jaffrès, H. Conditions for efficient spin injection from a ferromagnetic metal into a semiconductor. *Phys. Rev. B* **64,** 184420 (2001).
26. Smith, D. L. & Silver, R. N. Electrical spin injection into semiconductors. *Phys. Rev. B* **64,** 045323 (2001).
27. Mattana, R. *et al.* Electrical detection of spin accumulation in a *p*-type GaAs quantum well. *Phys. Rev. Lett.* **90,** 166601 (2003).
28. Bowen, M. *et al.* Spin-polarized tunnelling spectroscopy in tunnel junctions with half-metallic electrodes. *Phys. Rev. Lett.* **95,** 137203 (2005).
29. Soler, J. M. *et al.* The SIESTA method for ab initio order-N materials simulation. *J. Phys. Condens. Matter* **14,** 2745–2779 (2002).
30. Ferrari, V., Pruneda, J. M. A. & Artacho, E. Density functionals and half-metallicity in $La_{2/3}Sr_{1/3}MnO_3$. *Phys. Stat. Sol. a* **203,** 1437–1441 (2006).

Supplementary Information is linked to the online version of the paper at www.nature.com/nature.

Acknowledgements We thank G. A. J. Amaratunga, M. Bibes, H. Bouchiat, L. Brey, M. R. Buitelaar, M. J. Calderón, S. N. Cha, M. Chhowalla, A. Cottet, H. Jaffrès, D.-J. Kang, T. Kontos, P. Seneor and N. A. Spaldin. This work was funded by the UK EPSRC, NERC, BNFL, The Royal Society, the Spanish MEC (J.M.P.), Donostia International Physics Center (E.A.) and the EU.

Author Information Reprints and permissions information is available at www.nature.com/reprints. The authors declare no competing financial interests. Correspondence and requests for materials should be addressed to N.D.M. (ndm12@cam.ac.uk).